Some remarks on the stability coefficients and bubble stabilization of FEM on anisotropic meshes

STEFANO MICHELETTI[*]   SIMONA PEROTTO[*]
MARCO PICASSO[†]

Abstract

In this paper we re-address the anisotropic recipe provided for the stability coefficients in [13]. By comparing our approach with the residual-free bubbles theory, we improve on our a priori analysis for both the advection-diffusion and the Stokes problems. In particular, in the case of the advection-diffusion problem we derive a better interpolation error estimate by taking into account in a more anisotropic way the contribution associated with the convective term. Concerning the Stokes problem, we provide a numerical evidence that our anisotropic approach is thoroughly comparable with the bubble stabilization, which we study more in detail in our anisotropic framework.

Keywords:Anisotropic error estimates, advection-diffusion problems, Stokes problem, residual-free bubble functions, stabilized finite elements

1   Introduction

Stabilized finite elements like the Galerkin Least-Squares method (GLS), first introduced in [10] for solving the Stokes problem and in [3, 7, 11] for the approximation of the scalar advection-diffusion problem, are used in the finite element community in several application fields, such as viscoelastic flows, shells, magnetohydrodynamics and semiconductors. One of the advantages of such an approach is that in the case of the Stokes problem we can circumvent the classical inf-sup condition and use equal order approximation spaces for both the velocity and the pressure, e.g. continuous piecewise linear finite elements, while ensuring stability of the method by adding consistent terms to the weak formulation.

[*]MOX–Modeling and Scientific Computing, Dipartimento di Matematica "F. Brioschi", Politecnico di Milano, Via Bonardi 9, 20133 Milano, Italy (`mike@mate.polimi.it`, `simona@mate.polimi.it`).

[†]Département de Mathématiques, Ecole Polytechnique Fédérale de Lausanne, 1015 Lausanne, Switzerland (`marco.picasso@epfl.ch`).

The critical issue in stabilized finite elements is the design of the so-called stability coefficients weighting the extra terms added to the weak formulation. Typically, these coefficients, one for each element K of the triangulation, depend on some dimensionless number usually tuned on benchmark problems, and on a local mesh size, e.g. the triangle diameter h_K. A theoretical estimation of these quantities is proposed e.g. in [8, 9] for isotropic meshes.

Alternatively, the stabilization procedure based on residual-free bubbles relieves us of tuning any parameter provided that the residual-free bubble is accurately computed on each triangle (see e.g. [2, 17] and the references therein).

However, in the case of strongly anisotropic meshes the design of the stability coefficients is still an open question. In [14] numerical experiments show that good results can be obtained when using the minimum edge length of K instead of h_K. In [13] we propose a theoretical design of the stability coefficients suitable also for anisotropic meshes. Our analysis provides a general recipe for the definition of these coefficients valid for arbitrary shapes of the elements, taking into account a more detailed description of the geometrical structure of the triangles. To obtain this new definition we combine the a priori error analysis of [6, 7, 10] with the anisotropic interpolation estimates of [5]. However, this analysis is still unsatisfactory in the case of the advective dominated problem when the mesh is not well oriented with respect to the boundary layers, as the numerical results in Sect. 5.1 show.

In this paper, after addressing the main results of the analysis carried out in [13], we compare our anisotropic recipe with the definition of the stability coefficients provided by the residual-free bubbles theory. The main result is twofold: we first improve on the a priori analysis for the advection-diffusion problem carried out in [13] by analyzing in a more anisotropic way the interpolation error estimate associated with the convective term. Then we dwell on the Stokes problem and in particular we provide a numerical evidence that the two approaches actually coincide up to the tuning constant. Our numerical validation provides us with a practical numerical value for such a constant to use in the simulations.

The outline of the paper is as follows. In Sect. 2 we recall the anisotropic framework of [5, 13]. The a priori analysis leading to our definition of the stability coefficients for the advection-diffusion and Stokes problems is carried out in Sects. 3 and 4, respectively. Finally, in Sect. 5 we numerically compare our anisotropic recipes with the residual-free bubble ones. This analysis allows us to derive a better recipe than the one in [13] in the advective dominated case.

2   Anisotropic setting

In this section we summarize the leading ideas of the anisotropic analysis used for the design of the new stability coefficients.

Let $\Omega \subset \mathbb{R}^2$ be a polygonal domain and let $\{\mathcal{T}_h\}_h$ denote a family of conforming triangulations of $\overline{\Omega}$ into triangles K of diameter $h_K \leq h$, for any $0 < h \leq 1$. Let

$T_K : \widehat{K} \to K$ be the invertible affine mapping from a reference triangle $\widehat{K}$ into the general one K. The reference element $\widehat{K}$ can be indifferently chosen as, e.g., the unit right triangle $(0,0), (1,0), (0,1)$ or the equilateral one $(-1/2, 0), (1/2, 0), (0, \sqrt{3}/2)$. Let $M_K \in \mathbb{R}^{2 \times 2}$ be the nonsingular Jacobian matrix of the mapping T_K, i.e.

$$\mathbf{x} = T_K(\widehat{\mathbf{x}}) = M_K \widehat{\mathbf{x}} + \mathbf{t}_K \quad \text{for any } \widehat{\mathbf{x}} = (\widehat{x}_1, \widehat{x}_2)^T \in \widehat{K}, \tag{1}$$

with $\mathbf{t}_K \in \mathbb{R}^2$ and $\mathbf{x} = (x_1, x_2)^T \in K$.

The distinguishing feature of our anisotropic approach consists in exploiting the spectral properties of the mapping T_K itself in order to describe the orientation and the shape of each triangle K (see [5] for more details). With this aim, let us factorize matrix M_K via the polar decomposition as $M_K = B_K Z_K$, B_K and Z_K being symmetric positive definite and orthogonal matrices, respectively. Furthermore, B_K can be written in terms of its eigenvalues $\lambda_{1,K}, \lambda_{2,K}$ (with $\lambda_{1,K} \geq \lambda_{2,K}$) and of its eigenvectors $\mathbf{r}_{1,K}, \mathbf{r}_{2,K}$ as $B_K = R_K^T \Lambda_K R_K$, with

$$\Lambda_K = \begin{bmatrix} \lambda_{1,K} & 0 \\ 0 & \lambda_{2,K} \end{bmatrix} \quad \text{and} \quad R_K = \begin{bmatrix} \mathbf{r}_{1,K}^T \\ \mathbf{r}_{2,K}^T \end{bmatrix}.$$

Thus, the deformation of any $K \in \mathcal{T}_h$ with respect to $\widehat{K}$ can be measured by the so-called stretching factor $s_K = \lambda_{1,K}/\lambda_{2,K} (\geq 1)$.

Starting from the decompositions described above, new anisotropic interpolation error estimates have been derived for the Lagrange and Clément like interpolation operators. These estimates are an essential ingredient of the convergence analysis in the sections below, for both the advection-diffusion and Stokes problems. We refer to [5, 13] for the detailed derivation of these anisotropic interpolation error estimates. Let us introduce some anisotropic quantities related to this interpolation error analysis, which will be used in Sects. 3 and 4. Here and thereafter we use standard notation for Sobolev spaces, norms, seminorms and inner product [12]. For any function $v \in H^2(\Omega)$ and for any $K \in \mathcal{T}_h$, let

$$L_K^{i,j}(v) = \int_K \left(\mathbf{r}_{i,K}^T H_K(v) \, \mathbf{r}_{j,K} \right)^2 d\mathbf{x} \quad \text{for } i, j = 1, 2, \tag{2}$$

with $\left(H_K(v) \right)_{ij} = \partial^2 v / \partial x_i \partial x_j$ the Hessian matrix associated with the function $v|_K$. The quantities (2) can be interpreted as the square of the L^2-norm of the second-order directional derivatives of the function v with respect to the directions $\mathbf{r}_{i,K}$ and $\mathbf{r}_{j,K}$. Likewise, for any $v \in H^1(\Omega)$ and for any $K \in \mathcal{T}_h$, let $G_K(v)$ be the symmetric positive semi-definite matrix given by

$$G_K(v) = \sum_{T \in \Delta_K} \begin{bmatrix} \int_T \left(\dfrac{\partial v}{\partial x_1} \right)^2 d\mathbf{x} & \int_T \dfrac{\partial v}{\partial x_1} \dfrac{\partial v}{\partial x_2} d\mathbf{x} \\ \int_T \dfrac{\partial v}{\partial x_1} \dfrac{\partial v}{\partial x_2} d\mathbf{x} & \int_T \left(\dfrac{\partial v}{\partial x_2} \right)^2 d\mathbf{x} \end{bmatrix}, \tag{3}$$

3

where Δ_K is the patch of elements associated with the triangle K, that is the union of all the elements sharing a vertex with K. Throughout we assume the cardinality of any patch Δ_K as well as the diameter of the reference patch $\Delta_{\widehat{K}} = T_K^{-1}(\Delta_K)$ to be uniformly bounded independently of the geometry of the mesh, i.e., for any $K \in \mathcal{T}_h$,

$$\text{card}(\Delta_K) < \Gamma \quad \text{and} \quad \text{diam}(\Delta_{\widehat{K}}) = \widehat{C} \simeq O(1).$$

In particular, the latter hypothesis rules out some too distorted reference patches (see Fig. 1.1 in [13]).

3   The advection-diffusion problem

In this section we re-address in the framework of anisotropic meshes the crucial question of the choice of the stability coefficients for an advection-diffusion problem. We limit our analysis to the case of affine finite elements.

More in detail, in [13] we generalize the analysis in [7], where an expression for the stability coefficients is provided for both advective and diffusive dominated flows, to the case of possibly highly stretched elements. Thus, while [7] can be considered as the isotropic paradigm, our results can serve to design the stability coefficients in a more detailed way in an anisotropic context. With this aim, the convergence of the stabilized method is studied in a mesh dependent norm taking into account also the stability coefficients by requiring that the convergence rate, in both the advective and diffusive dominated regimes, be of maximal order. Theorem 3.1 provides the final result of this analysis.

Let us consider the standard advection-diffusion problem for the scalar field $u = u(\mathbf{x})$

$$\begin{cases} -\mu \, \Delta u + \mathbf{a} \cdot \nabla u = f & \text{in } \Omega, \\ u = 0 & \text{on } \partial\Omega, \end{cases} \tag{4}$$

where $\mu = \text{const} > 0$ is the diffusivity, $\mathbf{a} = \mathbf{a}(\mathbf{x}) \in (C^1(\overline{\Omega}))^2$ is the given flow velocity with $\nabla \cdot \mathbf{a} = 0$ in Ω, and $f = f(\mathbf{x}) \in L^2(\Omega)$ is the source term.

The variational formulation of problem (4) is: find a function $u \in H_0^1(\Omega)$ such that

$$B(u, v) = F(v) \quad \text{for any } v \in H_0^1(\Omega), \tag{5}$$

where $B(\cdot, \cdot)$ and $F(\cdot)$ define the bilinear and linear forms

$$B(u, v) = (\mu \, \nabla u, \, \nabla v) + (\mathbf{a} \cdot \nabla u, \, v) \quad \text{and} \quad F(v) = (f, \, v),$$

respectively, for any u and $v \in H_0^1(\Omega)$.

Let us discretize problem (5) by the GLS method as we are interested in advective dominated problems. The discrete problem thus is: find $u_h \in W_{h,0}$ which satisfies

$$B_h(u_h, \, v_h) = F_h(v_h) \quad \text{for any } v_h \in W_{h,0}, \tag{6}$$

4

with

$$B_h(u_h,\, v_h) = B(u_h,\, v_h)$$

$$+ \sum_{K \in \mathcal{T}_h} (-\mu\,\Delta u_h + \mathbf{a}\cdot\nabla u_h,\ \tau_K(-\mu\,\Delta v_h + \mathbf{a}\cdot\nabla v_h))_K, \tag{7}$$

$$F_h(v_h) = F(v_h) + \sum_{K \in \mathcal{T}_h} (f,\ \tau_K(-\mu\,\Delta v_h + \mathbf{a}\cdot\nabla v_h))_K,$$

where we let $W_{h,0} = W_h \cap H_0^1(\Omega)$, W_h being the finite element space comprising continuous affine elements. With this choice the terms $\Delta u_h|_K$ and $\Delta v_h|_K$ in (7) are identically equal to zero. Finally, we define the stability coefficients τ_K according to the theory in [7] as

$$\tau_K = \frac{\delta_K}{2} \frac{\xi(\mathrm{Pe}_K)}{\|\mathbf{a}\|_{L^\infty(K)}}, \tag{8}$$

where δ_K is a characteristic dimension of element K and the function ξ is defined as

$$\xi(\mathrm{Pe}_K) = \begin{cases} \mathrm{Pe}_K & \text{if} \quad \mathrm{Pe}_K < 1, \\ 1 & \text{if} \quad \mathrm{Pe}_K \geq 1. \end{cases} \tag{9}$$

This choice corresponds to considering a locally advective dominated flow when the element Péclet number

$$\mathrm{Pe}_K = \delta_K \frac{\|\mathbf{a}\|_{L^\infty(K)}}{6\,\mu}, \tag{10}$$

is greater than or equal to one. Notice that, while in [7] the choice $\delta_K = h_K$ is made up-front, on the contrary, in the presence of anisotropic meshes, this choice turns out not to be the optimal one. We provide below a more convenient choice of δ_K based on the error analysis.

3.1   Error analysis

To begin with, let us recall that the stabilized scheme (6) is consistent in the sense that if additional regularity is demanded for the solution u of the variational problem (5), that is $u \in H^2(\Omega) \cap H_0^1(\Omega)$, then the following relation holds

$$B_h(u,\, v_h) = F_h(v_h) \quad \text{for any } v_h \in W_{h,0}. \tag{11}$$

As a trivial consequence, simply by subtracting the equalities (11) and (6), we get the well-known Galerkin orthogonality property given by

$$B_h(u - u_h,\, v_h) = 0 \quad \text{for any } v_h \in W_{h,0}. \tag{12}$$

The convergence analysis in the sequel is derived in terms of the discrete norm $\|\cdot\|_h$ defined, for any $w \in H_0^1(\Omega)$, by

$$\|w\|_h^2 = \mu\,\|\nabla w\|_{L^2(\Omega)}^2 + \sum_{K \in \mathcal{T}_h} \|\tau_K^{1/2}\,\mathbf{a}\cdot\nabla w\|_{L^2(K)}^2. \tag{13}$$

In order to prove the convergence result of Theorem 3.1, let us begin with analyzing the stability and the continuity of the bilinear form $B_h(\cdot, \cdot)$. Concerning the stability, the following result can be stated.

Lemma 3.1 *For any $v_h \in W_{h,0}$,*

$$B_h(v_h, v_h) = \|v_h\|_h^2. \tag{14}$$

Thus (6) has a unique solution.

On the other hand, the continuity of the bilinear form $B_h(\cdot, \cdot)$ is provided by

Lemma 3.2 *For any $u \in H^2(\Omega) \cap H_0^1(\Omega)$ and for any $v_h \in W_{h,0}$, there exists a constant C such that*

$$
\begin{aligned}
|B_h(u, v_h)| \leq C &\left[\mu \|\nabla u\|_{L^2(\Omega)}^2 + \sum_{K \in \mathcal{T}_h} \left(\|\tau_K^{-1/2} u\|_{L^2(K)}^2 \right. \right. \\
&\left. \left. + \|\tau_K^{1/2} \mathbf{a} \cdot \nabla u\|_{L^2(K)}^2 + \|\tau_K^{1/2} \mu \Delta u\|_{L^2(K)}^2 \right) \right]^{1/2} \|v_h\|_h.
\end{aligned}
\tag{15}
$$

The stability and the continuity results (14) and (15), suitably combined with the anisotropic interpolation error estimates in [5, 13], are the basic ingredients to prove the anisotropic a priori error estimate below with respect to the norm $\| \cdot \|_h$ defined in (13).

Proposition 3.1 *Let $u \in H^2(\Omega) \cap H_0^1(\Omega)$ be the solution to (5) and let $u_h \in W_{h,0}$ be the solution to (6). Then there exists a constant C such that the a priori estimate*

$$
\begin{aligned}
\|u - u_h\|_h^2 \leq C \sum_{K \in \mathcal{T}_h} &\left\{ \left(\mu \mathcal{H}(1 - \mathrm{Pe}_K) \left[\frac{1}{\delta_K^2} + \frac{1}{\lambda_{2,K}^2} + \delta_K^2 \frac{(\lambda_{1,K}^2 + \lambda_{2,K}^2)^2}{\lambda_{1,K}^4 \lambda_{2,K}^4} \right] + \mathcal{H}(\mathrm{Pe}_K - 1) \right. \right. \\
&\left. \left. + \left[\frac{1}{\delta_K} + \frac{\delta_K}{\lambda_{2,K}^2} + \delta_K^3 \frac{(\lambda_{1,K}^2 + \lambda_{2,K}^2)^2}{\lambda_{1,K}^4 \lambda_{2,K}^4} \right] \|\mathbf{a}\|_{L^\infty(K)} \right) \left[\sum_{i,j=1}^2 \lambda_{i,K}^2 \lambda_{j,K}^2 L_K^{i,j}(u) \right] \right\}
\end{aligned}
\tag{16}
$$

holds true, with $L_K^{i,j}(u)$ defined as in (2) and where $\mathcal{H}(\cdot)$ is the Heaviside function given by

$$
\mathcal{H}(s) = \begin{cases} 0 & \text{if } s < 0 \\ 1 & \text{if } s > 0. \end{cases}
\tag{17}
$$

Sketch of the proof. The intermediate result

$$\|u - u_h\|_h^2 \leq C \sum_{K \in \mathcal{T}_h} \Big[\|\tau_K^{1/2} \, \mathbf{a} \cdot \nabla(u - r_K(u))\|_{L^2(K)}^2$$

$$+ \mu \, \|\nabla(u - r_K(u))\|_{L^2(K)}^2 + \|\tau_K^{-1/2} \, (u - r_K(u))\|_{L^2(K)}^2 \tag{18}$$

$$+ \|\tau_K^{1/2} \, \mu \, \Delta(u - r_K(u))\|_{L^2(K)}^2 \Big]$$

is a direct consequence of Lemmas 3.1 and 3.2, and of the Galerkin orthogonality (12), where $r_K(v)$ denotes the Lagrange W_h-interpolant of v, for any $v \in C^0(\Omega)$. The final result (16) follows from (18) combined with the interpolation error estimates of [5, 13].

We are now in position to state the main result of this section which represents the anisotropic counterpart of Theorem 3.1 in [7] in the case of affine elements.

Theorem 3.1 *Let $u \in H^2(\Omega) \cap H_0^1(\Omega)$ be the solution to (5) and let $u_h \in W_{h,0}$ be the solution to (6). Then the new (anisotropic) definitions of the stability coefficient and of the local Péclet number are*

$$\tau_K = \frac{\lambda_{2,K}}{2} \, \frac{\xi(\mathrm{Pe}_K)}{\|\mathbf{a}\|_{L^\infty(K)}}, \tag{19}$$

$$\mathrm{Pe}_K = \lambda_{2,K} \, \frac{\|\mathbf{a}\|_{L^\infty(K)}}{6 \, \mu}, \tag{20}$$

respectively, where $\xi(\cdot)$ is the same as in (9). Moreover, under this choice there exists a constant C such that it holds

$$\|u - u_h\|_h^2 \leq C \sum_{K \in \mathcal{T}_h} \Big\{ \lambda_{2,K}^2 \Big(\lambda_{2,K} \|\mathbf{a}\|_{L^\infty(K)} \mathcal{H}(\mathrm{Pe}_K - 1)$$

$$+ \mu \mathcal{H}(1 - \mathrm{Pe}_K) \Big) \big[s_K^4 L_K^{1,\,1}(u) + L_K^{2,\,2}(u) + 2 s_K^2 L_K^{1,\,2}(u) \big] \Big\},$$

where the quantities $L_K^{i,\,j}(u)$ and the function $\mathcal{H}(\cdot)$ are defined in (2) and (17), respectively.

Sketch of the proof. Let us rewrite the a priori error estimate (16) by introducing

the definition of the stretching factor s_K as

$$\|u - u_h\|_h^2 \leq C \sum_{K \in \mathcal{T}_h} \left\{ \left(\mu \mathcal{H}(1 - \text{Pe}_K) \underbrace{\left[\frac{\lambda_{2,K}^4}{\delta_K^2} + \lambda_{2,K}^2 + \delta_K^2 \frac{(\lambda_{1,K}^2 + \lambda_{2,K}^2)^2}{\lambda_{1,K}^4} \right]}_{(I)} \right. \right.$$

$$\left. + \mathcal{H}(\text{Pe}_K - 1) \underbrace{\left[\frac{\lambda_{2,K}^4}{\delta_K} + \delta_K \lambda_{2,K}^2 + \delta_K^3 \frac{(\lambda_{1,K}^2 + \lambda_{2,K}^2)^2}{\lambda_{1,K}^4} \right]}_{(II)} \|\mathbf{a}\|_{L^\infty(K)} \right) \tag{21}$$

$$\left. \underbrace{\left[s_K^4 \, L_K^{1,1}(u) + L_K^{2,2}(u) + 2 s_K^2 \, L_K^{1,2}(u) \right]}_{(III)} \right\}$$

where the term (III) is now equivalent to the H^2-norm of u on K, on recalling the definition (2) and that s_K is a dimensionless quantity. Moreover, no role is played by the term $(\lambda_{1,K}^2 + \lambda_{2,K}^2)^2 / \lambda_{1,K}^4$ since

$$1 < \frac{(\lambda_{1,K}^2 + \lambda_{2,K}^2)^2}{\lambda_{1,K}^4} \leq 4.$$

Let us first analyze the term (I) of (21). It turns out that the maximal order of convergence is obtained when all the three terms in (I) are of the same order. With this aim, setting $\delta_K \simeq \lambda_{1,K}^m \lambda_{2,K}^n$ for some $m, n \in \mathbb{Q}$, we find these values by requiring that all the three terms in (I) be of same order with respect to both $\lambda_{1,K}$ and $\lambda_{2,K}$. By doing so, we get $m = 0$ and $n = 1$, i.e. $\delta_K \simeq \lambda_{2,K}$. By a similar line of reasoning, it can be checked that the same value for δ_K is obtained for the term (II). It also turns out that, under the choice $\delta_K \simeq \lambda_{2,K}$, (I) behaves like $\lambda_{2,K}^2$ while (II) as $\lambda_{2,K}^3$. Having computed the value of δ_K, relations (19)-(20) follow immediately on recalling (8) and (10).

Notice that in the above proof the parameter δ_K is determined up to a constant. The definitions (19)-(20) are consistent with a choice of this constant equal to 1.

Remark 3.1 *In Sect. 5.1 we propose an alternative recipe to (19)-(20) and (9) starting from a more accurate interpolation error estimate.*

4 The Stokes problem

The results obtained in Sect. 3 can be easily extended to the case of the Stokes problem. In the very same spirit as in the advection-diffusion case, starting from the stabilized (GLS) formulation presented in [6, 10], we extend the convergence results obtained in Theorem 3.1 in [6] to the case of a general anisotropic mesh (see

Theorem 4.1).

Given the viscosity $\mu = \text{const} > 0$ and the source term $\mathbf{f} = \mathbf{f}(\mathbf{x}) \in (L^2(\Omega))^2$, we are looking for $\mathbf{u} = \mathbf{u}(\mathbf{x})$ and $p = p(\mathbf{x})$ such that

$$\begin{cases} -\mu \, \Delta \mathbf{u} + \nabla p = \mathbf{f} & \text{in } \Omega, \\ \nabla \cdot \mathbf{u} = 0 & \text{in } \Omega, \\ \mathbf{u} = \mathbf{0} & \text{on } \partial\Omega. \end{cases}$$

The corresponding variational formulation consists in finding $(\mathbf{u}, p) \in V \times Q$ such that

$$B(\mathbf{u}, p; \mathbf{v}, q) = F(\mathbf{v}, q) \quad \text{for any } (\mathbf{v}, q) \in V \times Q. \tag{22}$$

Here $V = (H_0^1(\Omega))^2$, $Q = L_0^2(\Omega)$ while $B(\cdot \, ; \, \cdot)$ and $F(\cdot)$ now are the symmetric bilinear and linear forms

$$B(\mathbf{u}, p; \mathbf{v}, q) = \mu(\nabla \mathbf{u}, \nabla \mathbf{v}) - (p, \nabla \cdot \mathbf{v}) - (q, \nabla \cdot \mathbf{u})$$

$$F(\mathbf{v}, q) = (\mathbf{f}, \mathbf{v})$$

respectively, for any $(\mathbf{u}, p)$, $(\mathbf{v}, q) \in V \times Q$.

As done in the advection-diffusion case, problem (22) is discretized by using the GLS method. The discrete problem consequently is: find $(\mathbf{u}_h, p_h) \in V_h \times Q_h$ which, for any $(\mathbf{v}_h, q_h) \in V_h \times Q_h$, satisfy

$$B_h(\mathbf{u}_h, p_h; \mathbf{v}_h, q_h) = F_h(\mathbf{v}_h, q_h), \tag{23}$$

where $V_h \times Q_h \subset V \times Q$ is the approximation space for velocity and pressure comprising continuous affine functions over $\mathcal{T}_h$. Here the symmetric bilinear form $B_h(\cdot \, ; \, \cdot)$ and the linear form $F_h(\cdot)$ are defined by

$$\begin{aligned} B_h(\mathbf{u}_h, p_h; \mathbf{v}_h, q_h) &= B(\mathbf{u}_h, p_h; \mathbf{v}_h, q_h) \\ &- \sum_{K \in \mathcal{T}_h} (-\mu \, \Delta \mathbf{u}_h + \nabla p_h, \tau_K(-\mu \, \Delta \mathbf{v}_h + \nabla q_h))_K, \\ F_h(\mathbf{v}_h, q_h) &= F(\mathbf{v}_h, q_h) - \sum_{K \in \mathcal{T}_h} (\mathbf{f}, \tau_K(-\mu \, \Delta \mathbf{v}_h + \nabla q_h))_K, \end{aligned} \tag{24}$$

with τ_K stability coefficients to be suitably chosen. Notice that the terms $\Delta \mathbf{u}_h|_K$ and $\Delta \mathbf{v}_h|_K$ in (24) are identically equal to zero due to the choice made for the finite element space V_h.

It is well-known that the GLS scheme (23) is consistent in the sense that if the solution $(\mathbf{u}, p) \in V \times Q$ of (22) is regular enough, i.e. if $(\mathbf{u}, p) \in (V \cap (H^2(\Omega))^2) \times (Q \cap H^1(\Omega))$, then for any $(\mathbf{v}_h, q_h) \in V_h \times Q_h$

$$B_h(\mathbf{u}, p; \mathbf{v}_h, q_h) = F_h(\mathbf{v}_h, q_h).$$

9

Consequently, if $(\mathbf{u}_h, p_h) \in V_h \times Q_h$ is the solution to (23) we obtain the Galerkin orthogonality property, i.e. for any $(\mathbf{v}_h, q_h) \in V_h \times Q_h$

$$B_h(\mathbf{u} - \mathbf{u}_h, p - p_h; \mathbf{v}_h, q_h) = 0.$$

As in Sect. 3.1, we introduce the discrete norm $\| \cdot \|_h$ defined, for any $(\mathbf{v}, q) \in V \times (Q \cap H^1(\Omega))$, by

$$\|(\mathbf{v}, q)\|_h^2 = \mu \|\nabla \mathbf{v}\|_{L^2(\Omega)}^2 + \sum_{K \in \mathcal{T}_h} \|\tau_K^{1/2} \nabla q\|_{L^2(K)}^2. \tag{25}$$

The convergence analysis has been carried out with respect to this norm. Following exactly the same steps as in Sect. 3.1 (see [13] for the details), we have:

Theorem 4.1 *Let* $(\mathbf{u}, p) \in (V \cap (H^2(\Omega))^2) \times (Q \cap H^1(\Omega))$ *be the solution to (22) and let* $(\mathbf{u}_h, p_h) \in V_h \times Q_h$ *be the solution to (23). Then the new (anisotropic) definition of the stability coefficients is*

$$\tau_K = \alpha \frac{\lambda_{2,K}^2}{\mu}, \tag{26}$$

where $\alpha \simeq O(1)$ *is the tuning constant. Moreover, under this choice there exists a constant* $C = C(\Gamma, \widehat{C}, \widehat{K})$ *such that it holds*

$$\|(\mathbf{u} - \mathbf{u}_h, p - p_h)\|_h^2 \leq C \sum_{K \in \mathcal{T}_h} \left\{ \lambda_{2,K}^2 \left(\mu \left[s_K^4 L_K^{1,1}(\mathbf{u}) + L_K^{2,2}(\mathbf{u}) + 2 s_K^2 L_K^{1,2}(\mathbf{u}) \right] \right. \right.$$
$$\left. \left. + \frac{1}{\mu} \left[s_K^2 (\mathbf{r}_{1,K}^T G_K(p) \mathbf{r}_{1,K}) + (\mathbf{r}_{2,K}^T G_K(p) \mathbf{r}_{2,K}) \right] \right) \right\},$$

where the quantities $L_K^{i,j}(\mathbf{u})$ *are a straightforward generalization of (2) to the vector case and* G_K *is the matrix defined in (3).*

Theorem 4.1 represents the anisotropic counterpart of Theorem 3.1 in [6] restricted to the case of (continuous) affine elements for both velocity and pressure. Moreover, we provide estimates in a different norm, namely the discrete norm $\| \cdot \|_h$ in (25), while in [6] the errors $\|\mathbf{u} - \mathbf{u}_h\|_{(H^1(\Omega))^2}$, $\|\mathbf{u} - \mathbf{u}_h\|_{(L^2(\Omega))^2}$ and $\|p - p_h\|_{L^2(\Omega)}$ are considered. Moreover, in Sect. 5.2 we suggest a practical value for α by comparing (26) with the corresponding bubble stabilization.

Remark 4.1 *The recipes (19) and (26) have been employed for an a posteriori error analysis in [15] and [4], respectively. In both cases, the numerical results assess the good behavior of the new anisotropic stability coefficients.*

5 Comparison with bubble stabilization

In the two following sections we compare the recipes (19) for the advection diffusion problem and (26) for the Stokes problem with their analogues provided by bubble stabilization.

5.1 The advection-diffusion problem

Let us address the more interesting advective dominated problem. The diffusive dominated case will be covered when dealing with the Stokes problem.
Let us recall that the residual-free bubble method gives

$$\tau_K^B \simeq \frac{h_a}{3 \left\| \mathbf{a} \right\|_{L^\infty(K)}} \tag{27}$$

where h_a is the longest triangle length in the streamline direction assuming $\mathbf{a}$ to be piecewise constant over the mesh (see e.g. [2, 17]). We have solved problem (4) with $\mu = 10^{-2}$, $\mathbf{a} = (1,0)^T$, $f = 1$, $\Omega = (0,1)^2$, completed with homogeneous mixed boundary conditions (i.e. Dirichlet and Neumann conditions on the vertical and horizontal sides, respectively). Figure 1 shows the numerical solution on a 20×1000 mesh consisting of right triangles for the choice (19) (crosses) and (27) (diamonds), and likewise Fig. 2 on a 40×1000 grid. Notice that in both cases the mesh is not correctly chosen, being mostly refined along the boundary layer. The recipe (19) is more unstable compared with (27), though the results improve when the mesh is correctly refined across the boundary layer.
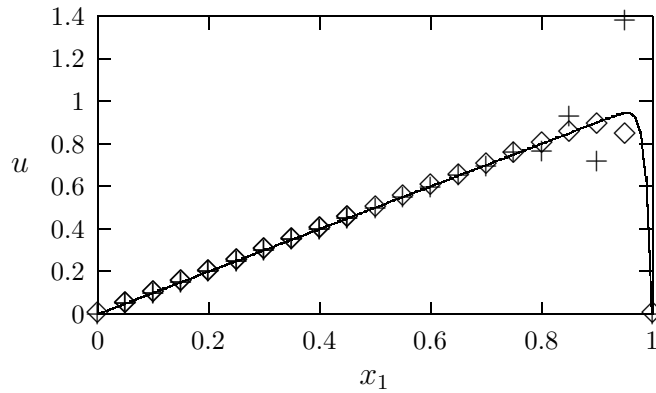
Figure 1: Computations on a 20×1000 mesh. Diamonds : τ_K as in (27); crosses : τ_K as in (19)

As a second test-case we have solved (4) with $\mu = 10^{-4}$, $\mathbf{a} = (2,1)^T$, $f = 0$, $\Omega = (0,1)^2$, completed with Dirichlet boundary conditions ($u = 1$ on the left and top sides and $u = 0$ on the remaining ones). In this case we have carried out an adaptive iterative procedure based on the a posteriori analysis in [15] implementing the recipe (19). Figure 3 shows on the top line the contour plot of the numerical solution and the final adapted mesh. In the middle line two zooms of the boundary layer are highlighted, 1000× and 10000×, respectively. On the bottom line we display two details of the internal layer obtained with an enlargement 100× and

11
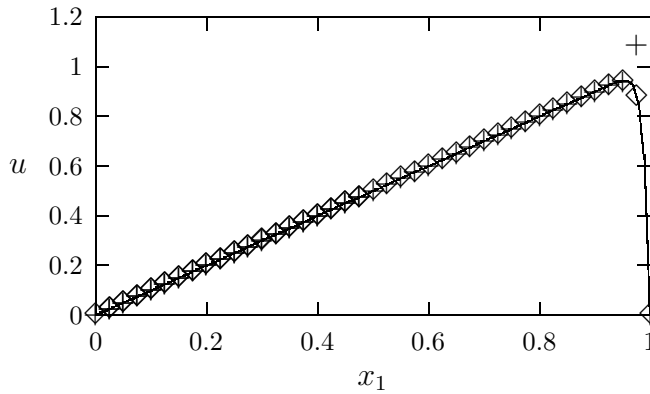
Figure 2: Computations on a 40×1000 mesh. Diamonds : τ_K as in (27); crosses : τ_K as in (19)

$1000\times$. Notice in particular how both boundary layers are very well captured by the final mesh whose triangles have a stretching factor as large as 10000.

These numerical tests show that our recipe and the free-residual bubbles one differ especially when the mesh in not suited for correctly resolving the anisotropic features of the solution, e.g. when the mesh is refined skew to a boundary layer (see Figs. 1-2). On the other hand, both recipes perform well when the mesh has the correct orientation, for example in the case of the internal layer in Fig. 3. In this case we do not show the results obtained using the bubble recipe since they are very similar to the ones shown in Fig. 3. Notice that in Figs. 1-2 the amount of stabilization introduced by our recipe, being proportional to $\lambda_{2,K}$, is much less than the one associated with the bubble stabilization as $\tau_K^B \simeq h_a \simeq \lambda_{1,K}$.

In Fig. 3 the mesh along the internal layer is very well oriented, being the narrowest dimension of the triangles placed across the layer, and, as in the former case, our recipe should introduce less stabilization with respect to the bubble stabilization. However, because we are in the presence of an internal layer, the streamline stabilization term $(\mathbf{a} \cdot \nabla u_h, \mathbf{a} \cdot \nabla v_h)_K$ in (7) is negligible, thus "killing" the effect of the different values of the τ_K's in the two cases. These considerations seem to indicate that the bubble stabilization is, in general, more robust than ours but that when the mesh is suited for the problem at hand both procedures give equally reasonable results (see Fig. 4). We point out that this discussion deals essentially with the a priori analysis or in general when one solves the problem at hand on a first guess mesh, in general not suited to the problem. When carrying out an adaptive procedure based on an a posteriori analysis we expect that this issue should be of no concern (see Fig. 3).

In the light of these numerical results we are prompted to looking for an improved recipe for the coefficients τ_K's, and in particular for a better definition of the local Péclet number. Actually, it is reasonable to expect that the Péclet number does
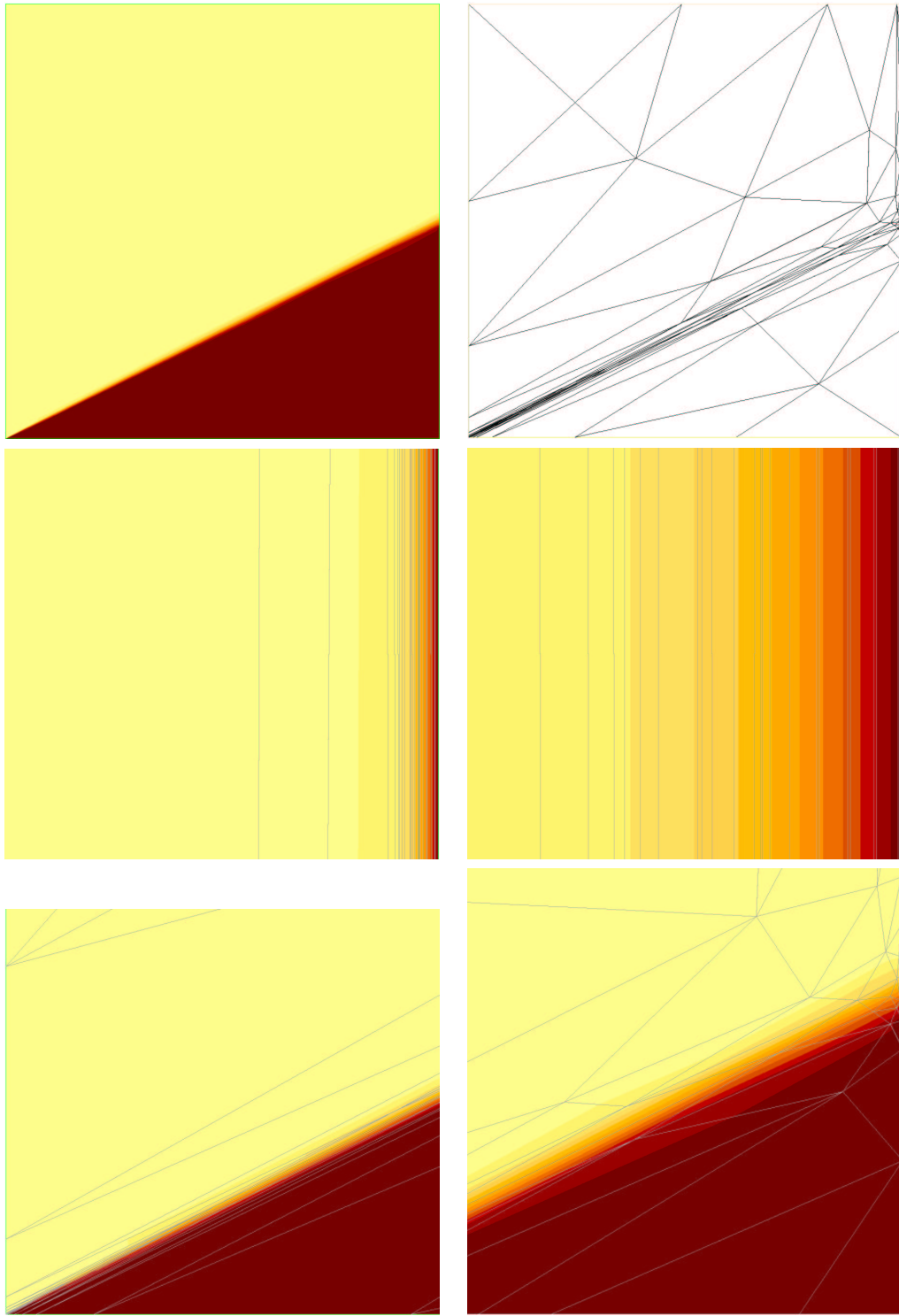
Figure 3: In top-down left-right order: contour plot, final adapted mesh, zoom 1000x, 10000x of the boundary layer, zoom 100x, 1000x of the internal layer for the second test-case using τ_K as in (19)
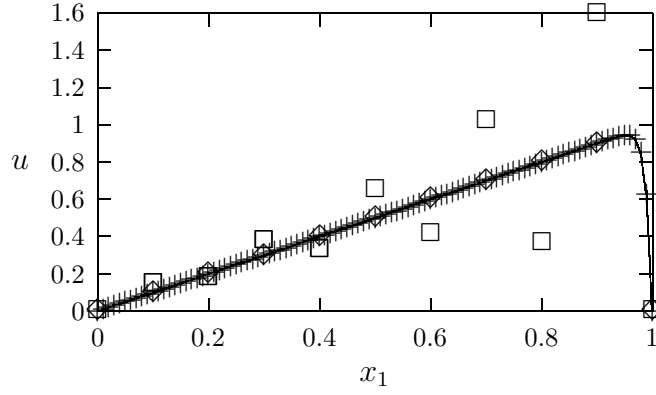
Figure 4: Computations with τ_K as in (19) on different anisotropic meshes. Squares: 10x10; diamonds: 100x10; crosses: 1000x10

depend on the direction of the convective field somehow. A possible remedy to this state of affairs could be obtained by improving the estimate of the interpolation error $||\tau_K^{1/2}\mathbf{a}\cdot\nabla(u-r_K(u))||_{L^2(K)}$ in (18) since this is the only term depending on convection. Let us now show how a more accurate estimate of this term can be obtained. As a consequence, we shall introduce the definition of a new quantity $\lambda_{a,K}$ relating the orientation of the triangle to the direction of the field $\mathbf{a}$. We have

$$
\begin{aligned}
||\tau_K^{1/2}\mathbf{a}\cdot\nabla(u-r_K(u))||_{L^2(K)}^2 &= \int_K [\tau_K^{1/2}\mathbf{a}\cdot\nabla(u-r_K(u))]^2\, d\mathbf{x} \\
&\leq \tau_K||\mathbf{a}||_{L^\infty(K)}^2 \int_K \left[\frac{\partial}{\partial a}(u-r_K(u))\right]^2 d\mathbf{x},
\end{aligned}
\tag{28}
$$

where we let $\partial v/\partial a = \mathbf{1}_a\cdot\nabla v$, for any $v\in H^1(\Omega)$, be the streamline derivative in the direction of field $\mathbf{a}$, $\mathbf{1}_a$ being its unit tangent vector. We are thus led to estimating the interpolation error of the streamline derivative and we obtain

$$
\begin{aligned}
\int_K \left[\frac{\partial}{\partial a}(u-r_K(u))\right]^2 d\mathbf{x} &= \int_K \left[\mathbf{1}_a\cdot\nabla(u-r_K(u))\right]^2 d\mathbf{x} \\
&= \lambda_{1,K}\lambda_{2,K}\int_{\widehat{K}} \left[\mathbf{1}_a\cdot(M_K^T)^{-1}\widehat{\nabla}(\widehat{u}-r_{\widehat{K}}(\widehat{u}))\right]^2 d\widehat{\mathbf{x}} \\
&= \lambda_{1,K}\lambda_{2,K}\int_{\widehat{K}} \left[\mathbf{1}_a^T R_K^T \Lambda_K^{-1} R_K Z_K \widehat{\nabla}(\widehat{u}-r_{\widehat{K}}(\widehat{u}))\right]^2 d\widehat{\mathbf{x}}
\end{aligned}
$$

14

$$= \lambda_{1,K}\lambda_{2,K} \int_{\widehat{K}} \left[(Z_K^T R_K^T \Lambda_K^{-1} R_K \mathbf{1}_a)^T \widehat{\nabla}(\widehat{u} - r_{\widehat{K}}(\widehat{u})) \right]^2 d\widehat{\mathbf{x}}$$

$$\leq \lambda_{1,K}\lambda_{2,K} \int_{\widehat{K}} \left| Z_K^T R_K^T \Lambda_K^{-1} R_K \mathbf{1}_a \right|^2 \left| \widehat{\nabla}(\widehat{u} - r_{\widehat{K}}(\widehat{u})) \right|^2 d\widehat{\mathbf{x}}$$

$$= \lambda_{1,K}\lambda_{2,K} \int_{\widehat{K}} \left| \Lambda_K^{-1} R_K \mathbf{1}_a \right|^2 \left| \widehat{\nabla}(\widehat{u} - r_{\widehat{K}}(\widehat{u})) \right|^2 d\widehat{\mathbf{x}} \tag{29}$$

$$\leq C_{\widehat{K}} \, \lambda_{1,K}\lambda_{2,K} \, ||\Lambda_K^{-1} R_K \mathbf{1}_a||^2_{L^\infty(\widehat{K})} \, |\widehat{u}|^2_{H^2(\widehat{K})}$$

$$= C_{\widehat{K}} \, ||\Lambda_K^{-1} R_K \mathbf{1}_a||^2_{L^\infty(K)} \sum_{i,j=1}^2 \lambda_{i,K}^2 \lambda_{j,K}^2 L_K^{i,j}(u),$$

where we have essentially used the decompositions of the matrix M_K in (1), the invariance of the euclidean norm $|\cdot|$ with respect to orthogonal matrices plus the identity

$$\lambda_{1,K}\lambda_{2,K} \, |\widehat{u}|^2_{H^2(\widehat{K})} = \sum_{i,j=1}^2 \lambda_{i,K}^2 \lambda_{j,K}^2 L_K^{i,j}(u)$$

proved in [5]. Notice that $C_{\widehat{K}}$ denotes a constant depending only on the reference triangle $\widehat{K}$. Let us delve into the quantity $||\Lambda_K^{-1} R_K \mathbf{1}_a||^2_{L^\infty(K)}$ in (29): we have

$$||\Lambda_K^{-1} R_K \mathbf{1}_a||^2_{L^\infty(K)} = \max_{\mathbf{x}\in K} |\Lambda_K^{-1} R_K \mathbf{1}_a(\mathbf{x})|^2 = \max_{\mathbf{x}\in K} \left| [\lambda_{1,K}^{-1} \mathbf{r}_{1,K}^T \mathbf{1}_a(\mathbf{x}), \, \lambda_{2,K}^{-1} \mathbf{r}_{2,K}^T \mathbf{1}_a(\mathbf{x})]^T \right|^2$$

$$= \max_{\mathbf{x}\in K} \left[\lambda_{1,K}^{-2} (\mathbf{r}_{1,K}^T \mathbf{1}_a(\mathbf{x}))^2 + \lambda_{2,K}^{-2} (\mathbf{r}_{2,K}^T \mathbf{1}_a(\mathbf{x}))^2 \right].$$

Notice that the above quantity is nothing but an averaged inverse squared characteristic length obtained by weighting $\lambda_{1,K}^{-2}$ and $\lambda_{2,K}^{-2}$ with the projection of $\mathbf{r}_{1,K}$ and $\mathbf{r}_{2,K}$, respectively in the direction of the convective field $\mathbf{a}$. Thus, we define the new quantity $\lambda_{a,K}$ such as

$$\lambda_{a,K}^{-2} = ||\Lambda_K^{-1} R_K \mathbf{1}_a||^2_{L^\infty(K)}. \tag{30}$$

Notice that we expect $\lambda_{a,K}$ to be the analogue of h_a in the case of the bubble stabilization.

Let us summarize the final error estimate concerning the advective term: from (28) and using definition (30) we obtain

$$||\tau_K^{1/2} \mathbf{a} \cdot \nabla(u - r_K(u))||^2_{L^2(K)}$$

$$\leq C_{\widehat{K}} \tau_K ||\mathbf{a}||^2_{L^\infty(K)} \, \lambda_{a,K}^{-2} \sum_{i,j=1}^2 \lambda_{i,K}^2 \lambda_{j,K}^2 L_K^{i,j}(u). \tag{31}$$

Remark 5.1 *We point out that in [13] we have obtained the analogue of estimate (31) but with $\lambda_{a,K}$ replaced by $\lambda_{2,K}$. Thus (31) represents an improvement over the old result because $\lambda_{2,K}$ is both independent of the convective field and always smaller than $\lambda_{a,K}$.*

In order to study the effect of this new estimate, let us first consider how the quantity $\lambda_{a,K}$ behaves in the two limiting cases when $\mathbf{a}$ is parallel to $\mathbf{r}_{1,K}$ or $\mathbf{r}_{2,K}$. It follows that $\lambda_{a,K} \equiv \lambda_{1,K}$ and $\lambda_{a,K} \equiv \lambda_{2,K}$, respectively so that $\lambda_{a,K}$ can always be identified with the characteristic dimension of the triangle in the streamline direction. Going back to the case of the problem exhibiting a boundary layer in Figs. 1-2 and 4, we expect the stability coefficient τ_K to depend on $\lambda_{a,K}$ when the problem is advective dominated, analogously to (27), while τ_K should approach the limiting value $\lambda_{2,K}^2/\mu$ in the diffusive dominated case (see also Sect. 5.2). This suggests defining the following modified recipe replacing (19) and (9) with

$$\tau_K = \frac{\lambda_{a,K}}{2} \frac{\xi(\mathrm{Pe}_K)}{||\mathbf{a}||_{L^\infty(K)}}, \tag{32}$$

$$\xi(\mathrm{Pe}_K) = \begin{cases} \dfrac{\lambda_{2,K}^2}{\lambda_{a,K}^2} \mathrm{Pe}_K & \text{if } \mathrm{Pe}_K < 1, \\ 1 & \text{if } \mathrm{Pe}_K \geq 1, \end{cases}$$

where the definition (20) of the local Péclet number becomes

$$\mathrm{Pe}_K = \lambda_{a,K} \frac{||\mathbf{a}||_{L^\infty(K)}}{6\mu},$$

the quantity $\lambda_{a,K}$ being defined in (30). The limiting values of the τ_K's from the above definitions reproduce the advective dominated and diffusive dominated cases, when $\tau_K \simeq \lambda_{a,K}/||\mathbf{a}||_{L^\infty(K)}$ and $\tau_K \simeq \lambda_{2,K}^2/\mu$, respectively. Figure 5 collects the results of solving the model convection diffusion problem (4) on the boundary layer case with $\mu = 10^{-5}$. On the left column we show the numerical solutions obtained with τ_K as in (19) (crosses), τ_K as in (27) (diamonds) and τ_K as in (32) (squares) on a 20×1000 (top), 20×2000 (middle) and 20×4000 (bottom) mesh, respectively. On the right column the solution obtained using (19) has been dropped with a corresponding reduction of the vertical axes range. Notice that although the mesh is refined in the wrong direction, the modified recipe based on $\lambda_{a,K}$ performs better than the old one (19).

Table 1: Test case 1: convergence rate of the error $||u - u_h||_h$ as a function of the mesh spacing across the boundary layer

N	20	40	80	160	320	640
$||u - u_h||_h$	0.95	0.38	0.17	0.091	0.045	0.022
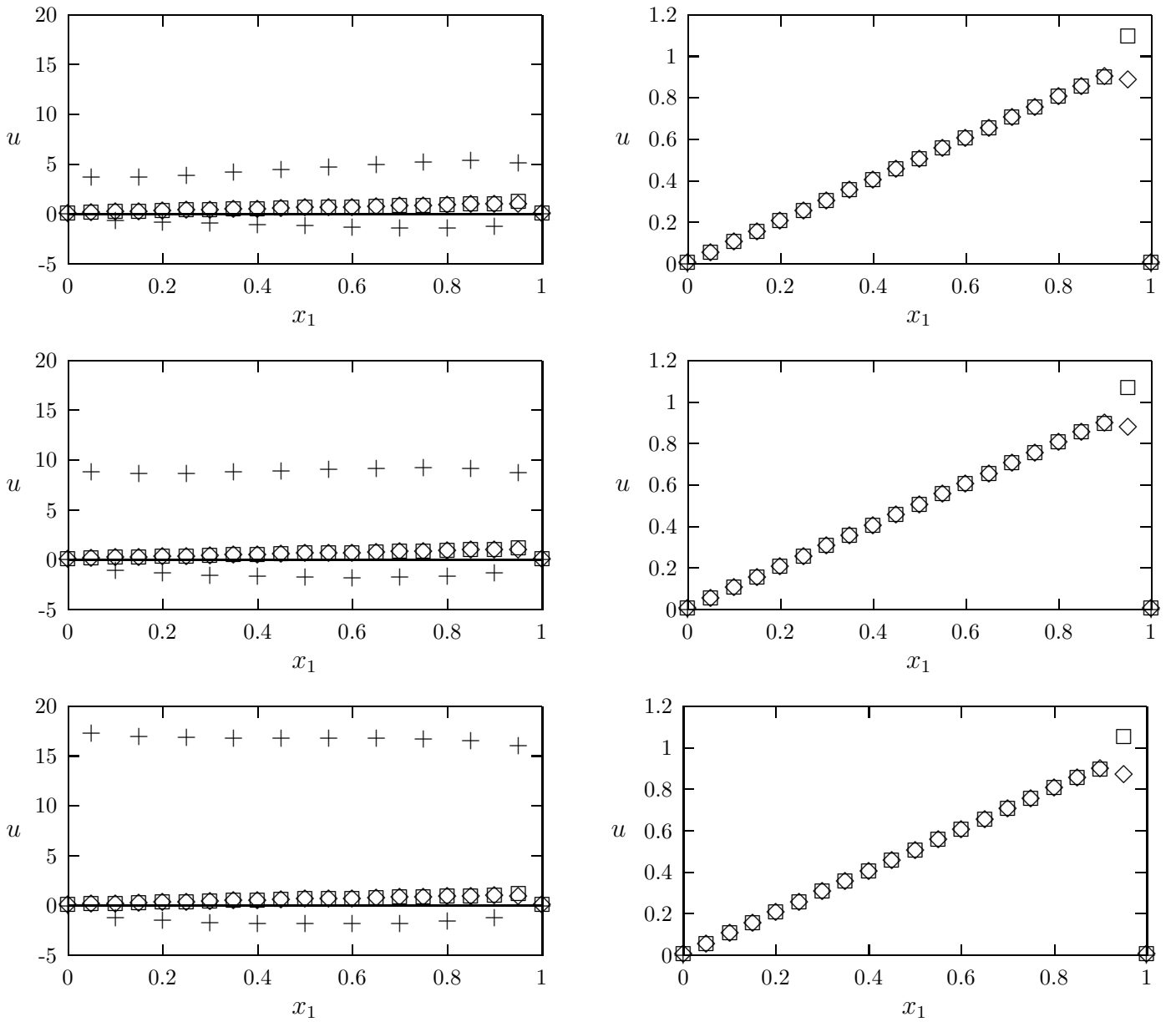
Figure 5: Left column: τ_K as in (19) (crosses), τ_K as in (27) (diamonds) and τ_K as in (32) (squares) on a 20×1000 (top), 20×2000 (middle) and 20×4000 (bottom) mesh. Right column: the same as in the left column but without the solution with τ_K as in (19)

To further prove this, we show in Table 1 the convergence behavior of the error $\|u - u_h\|_h$ as a function of the mesh dimension which is refined only in the horizontal direction. Notice that mesh consists of right triangles, with $N \times 4$ subdivisions in the horizontal and vertical directions, respectively. It can be appreciated that the

17

convergence rate is linear as happens in the case of the recipe based on (19) (see also Table 4.1 in [13]).

5.2 The Stokes problem

In this section we start from the definition of the stabilization coefficients provided e.g. in [2, 17] using the residual-free bubble approach in order to compare it with our anisotropic recipe (26). In particular, we carry out an extensive numerical assessment which shows that the two approaches actually coincide up to the constant α in (26), i.e. the τ_K's provided by the bubble recipe do exhibit the same dependence on $\lambda_{2,K}^2$ and μ as the one in (26). Moreover, our numerical analysis confirms that the constant α does not depend on the stretching factor s_K, at least for $s_K \gtrsim 10$, but only weakly on the stretching direction $\mathbf{r}_{1,K}$. This allows us to obtain a practical numerical value for α to use in the numerical simulations. The numerical and/or theoretical analysis of this constant has also been carried out e.g. in [1, 16, 18].

Let us recall that the residual-free bubble approach yields the choice

$$\tau_K^B = \frac{1}{|K|} \int\limits_K b_K(\mathbf{x}) \, d\mathbf{x} \tag{33}$$

for the stability coefficients, where b_K is the bubble solving the boundary value problem

$$\begin{cases} -\mu \, \Delta b_K = 1 & \text{in } K \\ b_K = 0 & \text{on } \partial K. \end{cases} \tag{34}$$

In the isotropic case it is known that $\tau_K^B \simeq h_K^2/\mu$. Hereafter we shall compute τ_K^B in the case of an arbitrarily shaped element. For this purpose, we have carried out two series of numerical experiments consisting in approximating the solution of problem (34) by a finite element procedure using affine elements over K, and then approximating (33) by the composite midpoint quadrature rule.

Table 2: $\theta = \frac{\pi}{4}, \alpha = 0.0647, a = 0.0204, b = 2.0000$

τ_K^B	1	2	3	4	5	6
10	0.0638	0.2553	0.5744	1.0212	1.5956	2.2977
20	0.0700	0.2798	0.6297	1.1194	1.7491	2.5186
40	0.0722	0.2886	0.6494	1.1546	1.8040	2.5978
80	0.0728	0.2912	0.6551	1.1646	1.8197	2.6204
160	0.0730	0.2918	0.6566	1.1672	1.8238	2.6262
320	0.0730	0.2920	0.6569	1.1679	1.8248	2.6277
640	0.0730	0.2920	0.6570	1.1680	1.8251	2.6281
1280	0.0730	0.2920	0.6570	1.1681	1.8251	2.6282

Table 3: $\theta = \frac{\pi}{2}, \alpha = 0.0365, a = 0.0105, b = 2.0000$

τ_K^B	1	2	3	4	5	6
10	0.0362	0.1448	0.3257	0.5790	0.9047	1.3028
20	0.0380	0.1519	0.3418	0.6076	0.9494	1.3671
40	0.0386	0.1543	0.3472	0.6172	0.9644	1.3887
80	0.0387	0.1550	0.3487	0.6198	0.9685	1.3946
160	0.0388	0.1551	0.3490	0.6205	0.9696	1.3962
320	0.0388	0.1552	0.3491	0.6207	0.9698	1.3966
640	0.0388	0.1552	0.3492	0.6207	0.9699	1.3967
1280	0.0388	0.1552	0.3492	0.6208	0.9699	1.3967

Table 4: $\theta = \pi, \alpha = 0.0366, a = 0.0121, b = 2.0000$

τ_K^B	1	2	3	4	5	6
10	0.0364	0.1454	0.3272	0.5818	0.9090	1.3090
20	0.0383	0.1533	0.3450	0.6133	0.9582	1.3799
40	0.0391	0.1562	0.3515	0.6248	0.9763	1.4059
80	0.0393	0.1571	0.3534	0.6282	0.9816	1.4135
160	0.0393	0.1573	0.3539	0.6291	0.9829	1.4154
320	0.0393	0.1573	0.3540	0.6293	0.9833	1.4159
640	0.0393	0.1573	0.3540	0.6294	0.9834	1.4161
1280	0.0393	0.1573	0.3540	0.6294	0.9834	1.4161

Without loss of generality we assume $\mu = 1$. The element K is obtained by mapping the reference unit right triangle $\widehat{K}$ using a simplification of T_K, i.e. $M_K = R_K^T \Lambda_K R_K$, that is neglecting the rotation associated with Z_K. For the first series of tests we have fixed the stretching direction of $\mathbf{r}_{1,K} = [\cos\theta, \sin\theta]^T$ (and thus of $\mathbf{r}_{2,K}$) and we have varied independently $\lambda_{2,K}$ and s_K. We summarize some of these results in Tables 2-4 where the values $\theta = \pi/4, \pi/2$ and π have been considered, respectively. The three tables show the values of the τ_K's as a function of $\lambda_{2,K}$ which varies across the columns and s_K varying across the rows. Notice that the computed values of τ_K seem to be independent of s_K while they do vary as a function of $\lambda_{2,K}$. To give a more quantitative estimate of these dependences, we have carried out a least-square procedure assuming a test function $\varphi_K = \alpha s_K^a \lambda_{2,K}^b$ with respect to the parameters α, a and b. The computed values appear on top of the tables and clearly suggest that the dependence of τ_K on $\lambda_{2,K}$ is quadratic while the dependence on s_K is almost negligible.
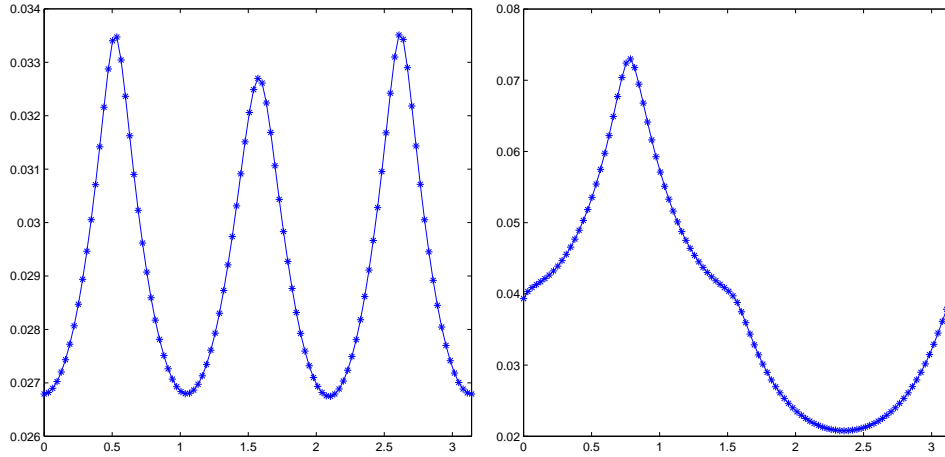
Figure 6: Constant α versus $\theta \in [0, \pi]$ for $\widehat{K}$ unit equilateral triangle (top) and $\widehat{K}$ unit right triangle (bottom)

The second series of numerical experiments aims at establishing the dependence of the constant α on the orientation of the triangle K given by $\mathbf{r}_{1,K}$. For this purpose, we have fixed the values of s_K and $\lambda_{2,K}$ and we have computed the values of α for different choices of $\theta \in [0, \pi]$ as $\alpha = \tau_K^B / \lambda_{2,K}^2$. We show in Figs. 6 the results of this investigation for both the unit equilateral and right triangle $\widehat{K}$, respectively. In both cases the range of the values of α is very narrow, being about 0.027-0.034 in the first case and 0.02-0.07 in the second one. This suggests that one could pick an average value $\alpha = \overline{\alpha} = 0.03$ and $\alpha = \overline{\alpha} = 0.04$, respectively. Preliminary results prove that these values for α are reasonable ([4]).

6   Conclusions

We have dealt with the design of the stability coefficients of Galerkin Least-Squares type FEM with emphasis on highly stretched meshes. We have studied the advection-diffusion and the Stokes problems for which we have devised theoretically sound stability coefficients based on anisotropic interpolation error estimates. We have also compared our recipes with their analogues from the residual-free bubbles approach. This comparison allows us to improve our stability coefficients in the case of advective dominated problems, while in the case of the Stokes problem we show that both approaches are identical up to the tuning constant. By a numerical assessment we compute this constant and we also improve on the residual-free bubbles stability coefficients for the Stokes problem highlighting their dependence on the shape of the mesh elements.

References

[1] Bank, R.E., Welfer, B.D.: A posteriori error estimates for the Stokes problem. SIAM J. Numer. Anal. 28, 591–623 (1991)

[2] Brezzi, F., Franca, L.P., Hughes, T.J.R., Russo, A.: $b = \int g$. Comput. Methods Appl. Mech. Engrg. 145, 329–339 (1997)

[3] Eriksson, K., Johnson, C.: Adaptive streamline diffusion finite element methods for stationary convection-diffusion problems. Math. Comput. 60, 167–188 (1993)

[4] Formaggia, L., Micheletti, S., Perotto, S.: An anisotropic mesh adaption procedure for CFD problems. (2002). In preparation

[5] Formaggia, L., Perotto, S.: New anisotropic a priori error estimates. Numer. Math. 89, 641–667 (2001)

[6] Franca, L.P., Stenberg, R.: Error analysis of some GLS methods for elasticity equations. SIAM J. Numer. Anal. 28, 1680–1697 (1991)

[7] Franca, L.P., Frey, S.L., Hughes, T.J.R.: Stabilized finite element methods. I. Application to the advective-diffusive model. Comput. Methods Appl. Mech. Engrg. 95, 253–276 (1992)

[8] Franca, L.P., Madureira, A.: Element diameter free stability parameters for stabilized methods applied to fluids. Comput. Methods Appl. Mech. Engrg. 105, 395–403 (1993)

[9] Harari, I., Hughes, T.J.R.: What are C and h?: inequalities for the analysis and design of finite element methods. Comput. Methods Appl. Mech. Engrg. 97, 157–192 (1992)

[10] Hughes, T.J.R., Franca, L.P., Balestra, M.: A new finite element formulation for computational fluid dynamics. V. Circumventing the Babuška-Brezzi condition: a stable Petrov-Galerkin formulation of the Stokes problem accommodating equal-order interpolations. Comput. Methods Appl. Mech. Engrg. 59, 85–99 (1986)

[11] Hughes, T.J.R., Franca, L.P., Hulbert, G.M.: A new finite element formulation for computational fluid dynamics: VIII. The Galerkin/least-squares method for advective-diffusive equations. Comput. Methods Appl. Mech. Engrg. 73, 173–189 (1989)

[12] Lions, J.L., Magenes, E.: Non-Homogeneous Boundary Value Problem and Application. Berlin: Springer-Verlag 1972

[13] Micheletti, S., Perotto, S., Picasso, M.: Stabilized finite elements on anisotropic meshes: a priori error estimates for the advection-diffusion and Stokes problems. SIAM J. Numer. Anal. (2002). Submitted

[14] Mittal, S.: On the performance of high aspect ratio elements for incompressible flows. Comput. Methods Appl. Mech. Engrg. 188, 269–287 (2000)

[15] Picasso, M.: An anisotropic error indicator based on Zienkiewicz-Zhu error estimator: application to elliptic and parabolic problems. SIAM J. Sci. Comput. (2002). Submitted

[16] Pierre, R.: Simple C^0 approximations for the computation of incompressible flows. Comput. Methods Appl. Mech. Engrg. 68, 205–227 (1988)

[17] Russo, A.: Bubble stabilization of finite element methods for the linearized incompressible Navier-Stokes equations. Comput. Methods Appl. Mech. Engrg. 132, 335–343 (1996)

[18] Tezduyar, T.E., Osawa, Y.: Finite element stabilization parameters computed from element matrices and vectors. Comput. Methods Appl. Mech. Engrg. 190, 411–430 (2000)